*Graphical Abstract

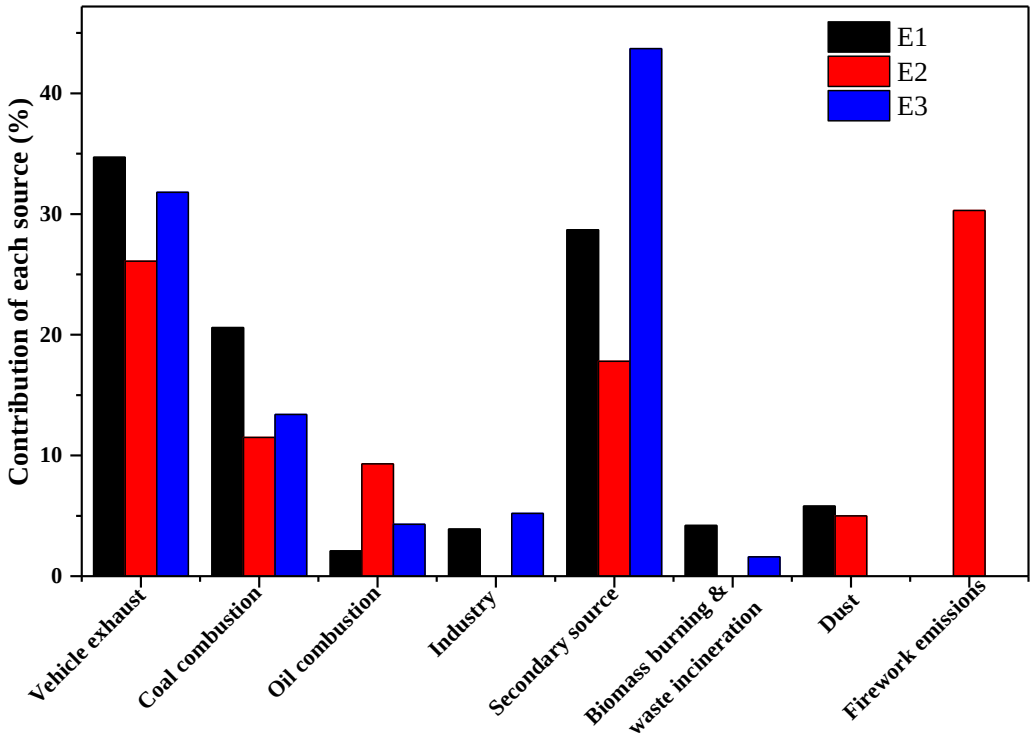

***Highlights (for review)**

- Measurement and source apportionment of $PM_{2.5}$ were performed during the 2015 Spring Festival (SF).
- Vehicular emission and secondary aerosol formation were identified as the dominant sources before the SF.
- During the SF fireworks were the largest contributor to the $PM_{2.5}$, accounting for 30%.
- Secondary aerosols became predominant after the SF with a contribution of 44% to the $PM_{2.5}$.
- Fireworks may pose a serious health problem to local residents.

Characterization and source identification of fine particulate matter in urban Beijing during the 2015 Spring Festival

Dongsheng Ji[1*], Yang Cui[1, 2], Liang Li[3], Jun He[4], Lili Wang[1], Hongliang Zhang[5], Wan Wang[6], Luxi Zhou[7], Willy Maenhaut[8], Tianxue Wen[1], Yuesi Wang[1*]

[1] *State Key Laboratory of Atmospheric Boundary Layer Physics and Atmospheric Chemistry, Institute of Atmospheric Physics, Chinese Academy of Sciences, Beijing, China.*

[2] *University of Chinese Academy of Sciences, Beijing, China*

[3] *China National Environmental Monitoring Center, Beijing, China*

[4] *Department of Chemical and Environmental Engineering, University of Nottingham Ningbo China, Ningbo, China*

[5] *Department of Civil & Environmental Engineering, Louisiana State University, USA*

[6] *State Key Laboratory of Environmental Criteria and Risk Assessment, Chinese Research Academy of Environmental Sciences, Beijing, China*

[7] *U.S. Environmental Protection Agency, Research Triangle Park, North Carolina, USA*

[8] *Department of Chemistry, Ghent University, Gent, Belgium*

* Corresponding authors

Email address: jds@mail.iap.ac.cn; wys@dq.cern.ac.cn

Abstract

The Spring Festival (SF) is the most important holiday in China for family reunion and tourism. During the 2015 SF an intensive observation campaign of air quality was conducted to study the impact of the anthropogenic activities and the dynamic characteristics of the sources. During the study period, pollution episodes frequently occurred with 12 days exceeding the Chinese Ambient Air Quality Standards for 24-h average $PM_{2.5}$ (75 μg/m^3), even 8 days with exceeding 150 μg/m^3. The daily maximum $PM_{2.5}$ concentration reached 350 μg/m^3 while the hourly minimum visibility was less than 0.8 km. Three pollution episodes were selected for detailed analysis including chemical characterization and diurnal variation of the $PM_{2.5}$ and its chemical composition, and sources were identified using the Positive Matrix Factorization model. The first episode occurring before the SF was characterized by more formation of SO_4^{2-} and NO_3^- and high crustal enrichment factors for Ag, As, Cd, Cu, Hg, Pb, Se and Zn and six categories of pollution sources were identified, whereby vehicle emission contributed 35% to the $PM_{2.5}$. The second episode occurring during the SF was affected heavily by large-scale firework emissions, which led to a significant increase in SO_4^{2-}, Cl^-, OC, K and Ba; these emissions were the largest contributor to the $PM_{2.5}$ accounting for 30%. During the third episode occurring after the SF, SO_4^{2-}, NO_3^- and NH_4^+ and OC were the major constituents of the $PM_{2.5}$ and the secondary source was the dominant source with a contribution of 44%. The results provide a detailed understanding on the variation in occurrence, chemical composition and sources of the $PM_{2.5}$ as well as of the gaseous pollutants affected by the change in anthropogenic activities in Beijing throughout the SF. They highlight the need for limiting the firework emissions during China's most important traditional festival.

Keywords: $PM_{2.5}$, firework emissions, source apportionment

1. Introduction

With the rapid development of economy, industrialization and urbanization during recent decades, air pollution has become a serious problem, which needs to be solved in China. Fine particulate matter (particulate matter with aerodynamic diameter less than 2.5 μm, $PM_{2.5}$) is the primary pollutant in most cities and attracts worldwide attention because of adverse effects on public health, visibility, air quality, and climate change (Chen et al., 2017; Cohen et al., 2017; Hu et al., 2015a; Lin et al., 2016; Liu et al., 2014b). In recent years, haze, which is closely related to elevated $PM_{2.5}$ concentrations, occurs frequently throughout China, causing serious health impacts, economic losses, and public complaints. So far, a series of the strictest measures for emission control have been issued and implemented to resolve the air pollution problem by the Chinese government from October 2013 (http://english.mep.gov.cn/News_service/news_release/index_26.shtml). The annual mean $PM_{2.5}$ concentrations in 2015 ranged from 22 to 107 $\mu g/m^3$ among the 74 key cities with an average value of 55 $\mu g/m^3$, exceeding the Chinese Ambient Air Quality Standards (CAAQS) Grade II annual mean of 35 $\mu g/m^3$ (Beijing environmental statement, 2015). The Beijing-Tianjin-Hebei region (BTH) is one of the most polluted areas, with an annual average $PM_{2.5}$ concentration of 77 $\mu g/m^3$ in 2015, approximately 2.2 times the CAAQS II threshold and 5.1 times the secondary air quality standard of the United States (annual mean: 15 $\mu g/m^3$) (https://www.epa.gov/pm-pollution/table-historical-particulate-matter-pm-national-ambient-air-quality-standards-naaqs). Thus, this region still faces severe challenges to mitigate $PM_{2.5}$ levels to meet both national and international regulations.

Beijing is the core city in the BTH region with the number of local residents being approximately 22 million and 273 million tourists visiting Beijing in 2015. As the capital city of China, the severe air pollution is of great concern because of its adverse health impacts on millions of local residents and foreigners working and travelling here (Guo et al., 2017). Significant emission control efforts have been made especially targeting key sources of concern to the reduce air pollution levels in Beijing. Although large improvement in air quality was made during important events, including the 2008 Olympic Games, the 2014 Asia-Pacific Economic Cooperation conference and the 2015 China Victory Parade Day (Jia et al., 2011; Wang et al., 2017; Wang et al., 2016; Xie et al., 2017), the $PM_{2.5}$ concentration did not decline substantially in

autumn and winter and the annual mean concentration was still approximately 80 μg/m^3 in 2015 (Beijing environmental statement, 2015). In particular, Beijing suffered 42 days of severe air pollution with an average value of 239 μg/m^3 in 2015. This indicated that current control measures might not be effective and that emission control efforts need to focus more accurately on the predominant sources during the pollution episodes. To further improve the air quality, it is necessary to characterize the $PM_{2.5}$ pollution episodes and to identify the sources of the $PM_{2.5}$.

Numerous studies have been initiated to investigate the evolution of the chemical composition of $PM_{2.5}$ and to identify the sources in Beijing (Hu et al., 2015b; Yu et al., 2013; Zhang et al., 2013). However, most source apportionment studies were based on continuous filter sampling (12 h or 24 h) and offline laboratory analysis (Liu et al., 2017a; Wang et al., 2016; Yao et al., 2016; Zong et al., 2016). The results reflected the average source contributions over different observation periods but could not shed light on the detailed variation of the air pollutants and the dynamic characteristics of the sources during severe pollution episodes, which last for short periods of less than one week. Thus, it is of great significance to analyze $PM_{2.5}$ and its chemical compositions in detail during severe episodes using near real-time data from state-of-the-art devices such as the Aerosol Mass Spectrometers (Elser et al., 2016), rapid collection of particles-ion chromatography systems (RCFP-IC) (Wen et al., 2006), semi-online OC and EC analyzers (Ji et al., 2016) and online multi-metal monitors (Gao et al., 2016), which used in combination allow one to determine the sources of the $PM_{2.5}$ (Gao et al., 2016; Jeong et al., 2016).

The Spring Festival (SF) is the most important holiday in China for family reunion and tourism. Extremely heavy traffic always occurs during this period because plenty of migrants, who work in megacities of China, go to their hometown before the SF and afterwards return back to work (Huang et al., 2012); besides, Beijing attracts approximately 10 million of tourists during the SF (http://travel.people.com.cn/n/2015/0226/c41570-26599014.html). Some of the industrial activities are temporarily halted so that the energy consumption decreases accordingly. However, intensive fireworks are held for celebration of the festival and they give rise to degradation in air quality (Huang et al., 2012; Ji et al., 2017; Kong et al., 2015). Some studies have focused on the effect of the SF holiday on the change in criteria air pollutants (SO_2, NO_x, CO, O_3, $PM_{2.5}$ and PM_{10}) (Dong et al., 2014; Jin et al., 2007) or the chemical composition of $PM_{2.5}$ (Feng et al., 2016; Huang et al., 2012; Kong et al., 2015; Tian et al., 2014; Wang et al., 2015). However, most of the

results solely focused on the variation in gaseous pollutants, PM or a special category of chemical species of $PM_{2.5}$ such as water-soluble inorganic ions, carbonaceous aerosols or trace elements and they made use of filter sampling and offline analysis. Thus, the variation in chemical composition and sources, which resulted from the dramatic change in anthropogenic activities including the emissions from the fireworks in a short-term period could not clearly be identified due to the low time resolution of the data or inadequate chemical information (Zou and Yao, 2014).

To fill this research gap, $PM_{2.5}$ and its chemical species including water-soluble inorganic ions, carbonaceous species and trace elements as well as major gaseous pollutants were concurrently measured on an hourly basis in Beijing from February 8 to March 2, 2015. The variation in $PM_{2.5}$ and its chemical species were determined, the sources were identified and the impact of the fireworks was evaluated. To our knowledge, this is the first time that near real-time instruments were jointly used to measure $PM_{2.5}$ and its chemical species in urban Beijing during the SF. The results provide valuable information for more effective $PM_{2.5}$ control in Beijing or other megacities in China during holidays.

2. Methodology

2.1. Sampling site and observation period

The sampling site (39°58′28″N, 116°22′16″E) is located inside the campus of the State Key Laboratory of Atmospheric Boundary Layer Physics and Atmospheric Chemistry, Institute of Atmospheric Physics (IAP), Chinese Academy of Sciences, in urban Beijing and is surrounded by busy urban roads (Fig. S1). The number of automotive vehicles in Beijing amounts to approximately 5.62 million and the average vehicular speeds within the urban traffic network were 28.1 and 25.1 km/h in 2015 during the morning and evening rush hours, respectively (All the data in this study on traffic, such as the traffic congestion index were obtained from http://www.bjjtw.gov.cn/bmfw /dljtyxqk/201503/t20150303_94290.html). Considering that a large number of industrial enterprises have been moved out of urban Beijing or phased out, there were no immediate industrial sources near the sampling site. However, small industrial sources and their possible operating schedules are unknown. The experimental campaign was conducted from February 8 to March 2, 2015, whereas the SF lasted for 7 days (from February 19 to 25). Air samples were collected at approximately 8 m above the ground. As shown in Table S1, the $PM_{2.5}$ concentrations at this site were significantly correlated with those at the 10 urban national sites,

including the Olympic center (Aoti), the Agriculture exhibition center (Nongzg), Dongsi (Dongs), the Temple of heaven (Tiant), Huayuan (Huay), Wanliu (Wanl), Gucheng (Guc), Guanyuan (Guany), Wanshouxigong (Wansxg) and Dingling (Dingl), which suggests that the sampling site is representative for urban Beijing. The locations of all the above sites were introduced in Cheng et al. (2015).

2.2. Instrumentation

To monitor $PM_{2.5}$ use was made of a synchronized hybrid ambient real-time particulate analyzer (Model 5030, Thermo-Fisher Scientific, Massachusetts, USA), which has been approved as a Federal Equivalent Method analyzer by the US EPA. The minimum detectable concentration limit was less than 0.2 $\mu g/m^3$ for 24 h. Operation, calibration and maintenance were strictly performed according to the instruction manual (https://tools.thermofisher.com/content/sfs/manuals/EPM-manual-Model%205030%20SHARP.pdf).

A RCFP-IC system was used to monitor SO_4^{2-}, NO_3^-, Cl^-, NH_4^+, K^+, Na^+, Ca^{2+} and Mg^{2+} hourly in $PM_{2.5}$. A semi-continuous organic carbon (OC) and elemental carbon (EC) field analyzer (Model 4, Sunset Laboratory Inc., Oregon, USA) with a modified NIOSH-like protocol was employed to obtain hourly OC and EC concentrations in $PM_{2.5}$. Detailed descriptions of the RCFP-IC system and the semi-continuous OC and EC analyzer were given in Wen et al. (2006) and Ji et al. (2016), respectively.

Hourly trace elements concentrations in $PM_{2.5}$ were obtained with an automated multi-metals monitor (Xact 625, Cooper Environmental Services, Oregon, USA). The quantification of the metals including K, Ca, Fe, Ag, Ba, As, Cd, Cu, Cr, Mn, Hg, Ni, V, Se, Zn, Ga, Pb, Co, Sn, Sb, Pd, Au and Tl in $PM_{2.5}$ was based on the US EPA method IO 3.3 using nondestructive energy-dispersive X-ray fluorescence. Operation, calibration and maintenance of the instrument were strictly performed according to its instruction manual (https://archive.epa.gov/nrmrl/archive-etv/web/pdf/p100cxcl.pdf). The stability of the automated multi-metals monitor was checked during every sampling and analysis cycle using an internal Pd rod.

Atmospheric temperature (T), relative humidity (RH), wind direction (WD) and wind speed (WS) were obtained using an automatic weather station (Model MILOS 520, VAISALA Inc., Finland) and atmospheric visibility was recorded via a visibility sensor (Model 6000, Belfort Instrument, Maryland, USA).

2.3. Source apportionment

Positive Matrix Factorization (PMF), which is an effective mathematical receptor model maintained by US EPA, is used worldwide for source apportionment. The principle and methodology of PMF have been reviewed and described in detail elsewhere (Han et al., 2017; Zíková et al., 2016; Zhang et al., 2013). The goal of the PMF model is to minimize the objective function *Q*:

$$Q = \sum_{i=1}^{n} \sum_{j=1}^{m} \left[\frac{x_{ij} - \sum_{k=1}^{p} g_{ik} f_{kj}}{u_{ij}} \right]^2$$

Where x_{ij} and u_{ij} are the concentration and uncertainty of the *jth* species in the *ith* sample, f_{kj} is the fraction of the *jth* species in *kth* source, g_{ik} indicates the contribution of the *kth* source to the *ith* sample, *p* is the number of sources, and *m* and *n* are the total number of species and samples, respectively. In this study, EPA's PMF version 5.0 (Norris et al., 2014) was used for source apportionment of the $PM_{2.5}$. Ca and K were measured by the automated multi-metals monitor and Ca^{2+} and K^+ by the RCFP-IC system, but the results from the former were selected for the source apportionment in this study. Thus, the PMF input dataset included $PM_{2.5}$, Cl^-, Na^+, Mg^{2+}, NH_4^+, SO_4^{2-}, NO_3^-, OC, EC, K, Ca, Fe, Ag, As, Cd, Ba, Cr, Cu, Mn, Ni, Hg, V, Se, Pb, and Zn. $PM_{2.5}$ was set as total variable. More information on the PMF as used in this study is given in the Supplementary material. The *Q*-values, source profiles and scaled residuals distributions were examined to obtain the most reasonable factor solution. The uncertainties of the PMF results were assessed by the displacement (DISP) and bootstrap (BS) error estimation methods with 100 BS runs and a minimum Pearson correlation coefficient of 0.6. In addition, the F_{peak} function was used to control the rotational ambiguity.

3. Results and discussion

3.1. Variations in air pollutants during the study period

Figs. 1(a) and 1(b) depict the hourly $PM_{2.5}$, SO_2, CO, NO_2 and O_3 concentrations and the hourly values of T, RH, WS, WD and visibility at the sampling site. As shown in Fig. 1(a), there were five typical cyclic accumulation processes of $PM_{2.5}$ recorded during the study period (Ji et al., 2012). High $PM_{2.5}$ concentrations were observed when southerly wind or calm wind prevailed while low concentrations were recorded during cold fronts accompanied by strong wind arriving in Beijing. The hourly concentrations of $PM_{2.5}$ varied from 3 to 430 μg/m^3 with an average of

115±107 μg/m^3. The daily averaged $PM_{2.5}$ concentrations ranged from 17 to 350 μg/m^3. There were 12 days for which the CAAQS 24-h Grade II standard for $PM_{2.5}$ (75 μg/m^3) was exceeded, even 8 days for which 150 μg/m^3 was exceeded. The highest hourly and daily $PM_{2.5}$ concentrations were recorded on February 15 before the SF; they were attributable to a combined effect of unfavorable meteorological conditions, heavy traffic caused by plenty of migrants going to their hometown (From February 4 to 15 the peak traffic congestion index was approximately 6.0, indicating that almost all major roads were congested) and residential heating. Compared to other studies conducted during SF periods, the daily average $PM_{2.5}$ concentration of 115±90 μg/m^3 in this study was slightly higher than those in Shanghai (Huang et al., 2012), Nanjing (Kong et al., 2015) and Xinxiang (Feng et al., 2016), but lower than those in Tianjin (Tian et al., 2014), Zhengzhou (Liu et al., 2014a) and Jinan (Yang et al., 2014) (Table S2). The hourly $PM_{2.5}$ concentrations at the IAP showed a similar variation as those observed in Tianjin, Shijiazhuang and Xingtai, which are major cities in the BTH region (Fig. S2), indicating that pollution episodes of a similar pattern occurred in different cities within the region during this period.

SO_2, CO and NO_2 showed a similar temporal variation as $PM_{2.5}$. The maximum hourly CO concentration, 6.6 mg/m^3, was observed on February 15 morning while that of NO_2 occurred on February 14 night, possibly because of continuing unfavorable meteorological conditions (low WS and high RH) and increased emissions from the high traffic intensity. The hourly maximum SO_2 concentration of 121 μg/m^3 was found at 1:00 on New Year's Eve (February 18); it was associated with firework emissions (Huang et al., 2012). Table S3 shows that SO_2, CO and NO_2 were significantly correlated with $PM_{2.5}$. SO_2 exhibited a high positive correlation with $PM_{2.5}$, suggesting that coal combustion and the firework emissions contributed a lot to the $PM_{2.5}$ (Ji et al., 2017). In contrast, O_3 was negatively correlated with the $PM_{2.5}$. That is because high $PM_{2.5}$ concentrations are usually accompanied with accumulation of primary pollutants (such as NO), which could consume O_3 (Han et al., 2011).

The whole campaign was divided into three periods: before the SF (from February 8 to 17), during New Year's Eve and the SF (from February 18 to 25) and after the SF (from February 26 to March 2). The average $PM_{2.5}$ mass concentrations and associated standard deviations before, during and after the SF were 138±123, 121±94 and 61±12 μg/m^3, respectively. The highest $PM_{2.5}$ concentration was recorded before the SF, followed by during and after the SF, consistent with the

decreasing strengths of anthropogenic emissions throughout the sampling period (Huang et al., 2012). That the lowest $PM_{2.5}$ level occurred after the SF could be due to favorable meteorological conditions and low emissions from anthropogenic sources since many migrant workers did not return to work immediately after the SF and the construction and industrial activities were not yet at their normal operational levels. A total of five pollution episodes was identified for the study period. They are listed in Table S4 of the Supplementary material; three of them were selected for detailed analysis in the following section.

3.2. Chemical characteristics of the three selected episodes

To better understand the evolution and sources of the air pollution throughout the festival period, three episodes were selected for further analysis as shown in Fig. 1(a) (shaded and gridded areas). The first episode (E1) was recorded from February 8 to10 before the SF. The second episode (E2) was observed from February 17 to 19 during the SF (February 18 was the Chinese New Year's Eve and February 19 was the first day of the SF). The third episode (E3) was recorded from February 27 to March 1 after the SF, when the holiday was ending and migrant workers and students gradually returned, which reflects the transition period from slightly to fully operational industrial activities. Note that the pollution episode occurring during February 13-15 was not selected as the multi-metals monitor did not work properly then.

3.2.1. E1 before the SF

Fig. 2 shows the hourly concentrations of the $PM_{2.5}$ constituents during E1. From 15:00 on February 8, NO_3^-, NH_4^+, SO_4^{2-}, Cl^-, OC and EC started to rise and they peaked at approximately 1:00 on February 10. The highest concentrations of SO_4^{2-}, NO_3^-, NH_4^+, Cl^-, OC and EC reached 27, 39, 23, 11.9, 57 and 9.0 $\mu g/m^3$, respectively. During the rapid increase stage, the increment rates of NO_3^-, NH_4^+, SO_4^{2-}, Cl^-, OC and EC were 0.7, 0.5, 0.4, 0.3, 1.4 and 0.2 $\mu g/m^3/h$, respectively. OC had the highest rate and a significant correlation between OC and EC with a slope of 6.3 was recorded, which reflects a combined contribution from vehicular exhaust, coal combustion, and biomass burning (Cao et al., 2005). Usually the SF travel rush starts 1-2 weeks before the SF and intensive traffic activities result in high OC and NO_3^- contributions to the $PM_{2.5}$, as observed in previous research (Huang et al., 2012; Kong et al., 2015). The significant correlation between OC

and CO (R^2=0.81) further corroborates the impact of vehicle emissions.

The atmospheric transformation of SO_2 to SO_4^{2-} and of NO_2 to NO_3^- could be calculated by the sulfur oxidation ratio (*SOR*) and nitrogen oxidation ratio (*NOR*) based on equations (1) - (3):

$$SOR = n[\text{nss-}SO_4^{2-}]/(n[SO_2] + n[\text{nss-}SO_4^{2-}]) \quad (1)$$

$$[\text{nss-}SO_4^{2-}] = [SO_4^{2-}]\text{-}0.2517\times[Na^+] \quad (2)$$

$$NOR = n[NO_3^-]/(n[NO_2]+ n[NO_3^-]) \quad (3)$$

where nss-SO_4^{2-} denotes non-sea-salt sulfate and the unit for *n* is mole/m^3; 0.2517 is the ratio of SO_4^{2-} to Na^+ in sea water (Tao et al., 2009). During the rapid increase stage, *SOR* and *NOR* were 0.13 and 0.17, suggesting rapid gas-particle transformation (Zhang et al., 2016). The NO_3^-/SO_4^{2-} mass ratio can be used to discuss the contributions of stationary and mobile sources (Feng et al., 2016). The average NO_3^-/SO_4^{2-} ratio of 1.6±0.7 suggests that the vehicle contribution was significantly larger than that from coal combustion during E1; this is consistent with the result obtained by PMF shown in Fig. 5.

K, Ca, Fe and Zn were the major elemental constituents with average concentrations of 1,340±360, 158±58, 360±110 and 240±100 ng/m^3, respectively (Table 1). Before 15:00 on February 8, all elements showed opposite variation patterns compared with the pattern for secondary inorganic aerosol (see Fig. 2). This could mainly be due to the significant contribution of elements from windblown dust (Shen et al., 2016), as is supported by high wind speeds shown in Fig. 1(b). Whereas most crustal matter and urban road dust contains a K/Fe ratio of less than 1.0, much higher ratios were noted during the evening and early morning hours (approximately 5:1) and they were still elevated during the day (approximately 2:1) (Chan et al., 1997). This might suggest a contribution from biomass burning at that time. During the accumulation process, Pb, Zn, As and Se showed an increased contribution with average concentrations of 98±6, 240±100, 29±10 and 5.3±1.4 ng/m^3, respectively; these elements are closely related with combustion (Pokorná et al., 2016). It suggests that coal combustion used for heating was still important during this episode.

The degree of enrichment relative to soil crustal matter for trace elements can be quantitatively assessed by the crustal Enrichment Factor (*EF*) based on equation (4):

$$EF = (X/X_{Ref})_{aerosol}/(X/X_{Ref})_{soil} \quad (4)$$

where *X* is element of interest and X_{Ref} is the reference element in soil (Huang et al., 2012; Liu et

al., 2017a). In this study, Fe in background soil in China was chosen as the reference element (Wei et al., 1991). The average *EF* values for elements in the three episodes are given in Table S5. Elements with *EF* values smaller than 10, which are usually considered to originate primarily from natural sources (Xu et al., 2013) included K, Fe, Ca, Cr, Mn and Ba during E1. Anthropogenic elements including Cu, As, Zn, Pb, Se, Ag, Hg and Cd had *EF* values higher than 100, ranging from 168 (Cu) to 10100 (Cd), suggesting the importance of anthropogenic sources. Note that the *EF* values of the elements declined during the rapid increase stage except for Ag and Cd, suggesting that these elements were not associated with the main cause of the $PM_{2.5}$ increase. Additionally, it was found that the *EF* values of Ni and V were higher than 10 during 4:00-7:00 on February 8 and 8:00-17:00 on February 10; this could be due to a substantial contribution from heavy oil combustion for these two elements (Dall'Osto et al., 2013).

3.2.2. E2 during the SF

Fig. 3 shows the temporal variation of the $PM_{2.5}$ constituents during E2 and Table 1 presents their average concentrations and associated standard deviations. Due to increased wind speed from the northwest or northeast varying from 2.2 to 5.2 m/s and because of a decline in anthropogenic emissions (i.e., from industries and vehicles), the concentrations $PM_{2.5}$ and its chemical species declined before 18:00 on February 18. The average visibility was 46±6 km. With the shift of WD from north to south and the decrease of WS, a $PM_{2.5}$ peak was recorded from 22:00 on February 17 to 2:00 on February 18 and as a result SO_4^{2-}, NO_3^-, NH_4^+, Cl^-, OC and EC peaked. Afterwards, the hourly $PM_{2.5}$ concentrations began to decrease until 18:00 on February 18 (New Year's Eve). Then the $PM_{2.5}$ concentrations increased quickly from 33 to 400 μg/m^3 and peaked at 1:00 on February 19 when huge amounts of firework emissions occurred. The time period with $PM_{2.5}$ concentrations of more than 75 μg/m^3 lasted for 70 h after the fireworks.

The highest concentrations of OC, EC, Cl^-, NO_3^-, SO_4^{2-}, K^+, NH_4^+, Na^+ and Mg^{2+} were 20, 2.1, 57, 12.6, 92, 96, 9.1, 2.2 and 5.9 μg/m^3 at 1:00 on February 19. K^+, SO_4^{2-} and Cl^- increased at fast rates of 13.3, 11.5 and 7.7 μg/m^3/h, respectively. These increases result from the fact that firework materials are made up of sulfur powder, carbon powder and $KClO_4$ (Ji et al., 2017). $KClO_4$ acts as the major oxidizer and the corresponding chemical reaction (R1) results in high Cl^- and SO_4^{2-} concentrations during the firework. In addition, potassium sulfate is also used as an

additive in the firework (Perry, 1999).

$$KClO_4 + S + C \rightarrow SO_2 + K_2SO_4\ (SO_2) + KCl + CO_2\ (CO) \quad \text{(R1)}$$

$$\sum Anions = [SO_4^{2-}]/48 + [NO_3^-]/62 + [Cl^-]/35.5 + [F^-]/19 \quad (5)$$

$$\sum Cations = [NH_4^+]/18 + [Mg^{2+}]/12 + [Ca^{2+}]/20 + [Na^+]/23 + [K^+]/39 \quad (6)$$

The $\sum Cations/\sum Anions$ molar ratio was 0.97 for the period from 19:00 on February 18 to 1:00 on February 19, which indicated that there was a slight deficiency in cations to neutralize the anions. A NO_3^- peak did not occur, in contrast to what was the case for K^+, SO_4^{2-} and Cl^-. This is because NO_3^- is not a major constituent of firework materials and the meteorological conditions were not favorable for secondary formation of NO_3^-. Note that the PM, which originates from fireworks can remain in the atmosphere for a long time and may be a substrate for heterogeneous reactions of SO_2 and NO_2, thus degrading air quality when favorable meteorological conditions prevail (Kong et al., 2015). As reported by Pathak et al. (2009), NO_3^- is preferably formed in an ammonia-deficient atmosphere via (R S4) in the Supplementary material, for which basically heterogeneous hydrolysis of N_2O_5 occurs on the moist surface of aerosols. The PM emitted by the fireworks during the SF provides an appropriate interface to form NO_3^- via heterogeneous reactions when the RH increases.

The correlations between OC and CO and between OC and EC were significant during E2. Furthermore, high OC/EC ratios (on average 9.2±5.3) were observed, which possibly result from the adhesive organic matter in the firework materials and in addition from vehicular exhaust and coal combustion. As shown in Fig. 3, K, Ba, Ca, Fe, Pb and Cu increased at rates of 870, 14.2, 10.1, 9.4, 4.7 and 4.7 ng/m^3/h, respectively, during the intensive firework emission period (from 19:00 on February 18 to 1:00 on February 19). The *EF* values of K, Ba, Cu and Pb reached 29, 22, 129 and 210, respectively, at 1:00 on February 19. The Ba, Cu and Pb concentrations increased by factors of 3.4, 5.6 and 1.8, respectively, in a short time, which could pose health risks to the local residents, in particular to children (Hamad et al., 2016). The average Ba concentration (99 ng/m^3) during the intensive emission period was higher than that observed in Nanjing during the Spring Festival (70 ng/m^3) (Kong et al., 2015). The results indicate that fireworks lead to substantial emissions of its related elements.

3.2.3. E3 after the SF

As shown in Fig. 4, SO_4^{2-}, Cl^-, NO_3^-, NH_4^+, OC and EC varied similarly to $PM_{2.5}$ with average concentrations of 15.4±15.8, 2.6±2.2, 12.0±12.8, 12.2±13.9, 12.6±9.7 and 1.6±1.4 μg/m^3, respectively. Compared to E2, the NO_3^- and NH_4^+ concentrations were much higher during E3. After the SF, migrant workers gradually returned to Beijing for work and traffic flows and industrial activities increased progressively. The emission intensities of various sources changed and the ratios of NO_3^-, SO_4^{2-} and NH_4^+ to total $PM_{2.5}$ varied correspondingly. The ratios of $NO_3^-/PM_{2.5}$, $SO_4^{2-}/PM_{2.5}$ and $NH_4^+/PM_{2.5}$ were 0.18±0.08, 0.29±0.21 and 0.17±0.08, respectively. During E3, the ratio of ∑Cations/∑Anions was 1.4 (with R^2=0.98 between both sums), indicating that the $PM_{2.5}$ was alkaline, which was different from that during the intensive firework emission period. A significant correlation was found between OC and EC was with a slope of 6.4 and a R^2 of 0.87. The high OC/EC ratios were related to the combined contributions from vehicular exhaust and coal combustion (Cao et al., 2005).

The average concentrations of K, Fe, Zn, and Ca were 410±170, 87±40, 36±19 and 34±18 ng/m^3, respectively, and aggregately these four elements accounted for 88.8% of the mass of all elements in this episode. As shown in Table S5, the *EF* values of Cd, Ag, Hg, Se, Pb, Zn, Cu, Ni, As and V were all higher than 10, indicating a quite important contribution for these elements from anthropogenic emissions. In contrast to what was the case in E2, the average *EF* values of elements related to industries like Cr, Cu, Zn, Hg and Pb increased during E3, which seems to reflect the progressive re-opening of the industrial activities.

The diurnal variation in $PM_{2.5}$ and its chemical constituents during E1, E2 and E3 was also examined; it is shown in the Supplementary material (Figs. S3, S4 and S5). Due to the influence of different source strengths, the diurnal variation was in accordance with the morning and evening rush hours and nighttime emissions as well as the additional emission from the fireworks during the SF.

3.3. Source apportionment of $PM_{2.5}$ for the three selected episodes

The PMF model was run 100 times with a random seed and the lowest *Q* was considered as base run solution. After examination of the F_{peak} values, the base run results (F_{peak} = 0) were retained for the three selected episodes. Mg^{2+} was excluded from the input of the model for E1 and

E3 because of lower signal-to-noise ratios and Ag and Cd were excluded for all three selected episodes due to the lower coefficients between measured and predicted values ($R^2 < 0.01$). Cr and Na^+ were also excluded for E2 and E3 because of poor match between the modeled and measured values, respectively. The PMF solutions with from four to eight factors were examined. The detailed solution analysis is presented in the Supplementary material. Seven, six and six factors were found to be reasonable for E1, E2 and E3, respectively.

Fig. 5 presents the seven identified source profiles and their average contributions to the $PM_{2.5}$ for E1. Factor 1 with high loadings of Ca, Cr, Mn, Fe and Zn was identified as dust because of the presence of the crustal elements Ca, Mn, and Fe. Ba, Cu, As, Se, Hg and Pb were also found in this factor. Road dust, windblown dust and construction dust could not be distinguished from each other because of the insufficient tracers for dust. Dust was an important source of $PM_{2.5}$ with an average contribution of 5.8%. Factor 2 was termed a source associated with vehicle exhaust because it is characterized by high loadings of NO_3^-, NH_4^+, OC and EC (Liu et al., 2017b; Singh et al., 2016; Zong et al., 2016). It is well known that vehicular emissions provide a substantial contribution to the OC and EC levels and that NH_4^+ is emitted by vehicles that are equipped with three-way catalytic converters (Chang et al., 2015). This source contributed with 35% to the $PM_{2.5}$ during E1, which is in accordance with the SF travel rush. Factor 3 was identified as coal combustion, as it is characterized by high Cl^-, OC and EC loadings. The high Cl^- loading associated with coal combustion in winter is a distinctive feature in Beijing and inland China (Liu et al., 2017b; Zhang et al., 2013). The contribution of coal combustion to the $PM_{2.5}$ was 21%. Factor 4 can be determined as secondary sources because of the high loadings of NO_3^-, NH_4^+, and SO_4^{2-}. This factor provided a contribution of 29% to the $PM_{2.5}$. Factor 5 has high loadings for V and Ni, which are related with oil combustion (Wang et al., 2016); it contributed with 2.1% to the $PM_{2.5}$. The sixth factor stood for industrial sources; it is characterized by a higher loading of Cu, Zn and As as well as a moderate loading of Hg, Pb and Cr (Wang et al., 2016; Yao et al., 2016). Since there are no industries in Beijing and because of the temporary shutdown of manufacturing in the surrounding areas of Beijing around the time of the SF, the industrial source only contributed with 3.9% during E1. Factor 7, characterized by a high loading of K and accounting for 4.2% of the $PM_{2.5}$, was biomass burning and waste incineration (Betha et al., 2014). As, Se, Hg and Pb also had a moderate loading in factor 7; the latter elements are also related with biomass

396 burning and waste incineration (Dall'Osto et al., 2013).

397 For E2, the six-factor solution provided the most physically reasonable source profiles.
398 Factor 1 was considered as vehicular exhaust, as it is characterized by high loadings of NO_3^-,
399 NH_4^+, OC and EC (see Fig. 6); it contributed with 26% to the $PM_{2.5.}$ Factor 2 had high loadings of
400 NO_3^-, NH_4^+ and SO_4^{2-} and was therefore identified as secondary sources but it is also partly related
401 to aging processes of firework emissions because it shows some loading of Ba, Cu and K (Kong et
402 al., 2015). This source contributed with 17.8% to the $PM_{2.5}$. Factor 3 was dust, characterized by
403 high Ca, Mn, Fe, Se, Ba and Pb, and it provided a contribution of 5%. Note that dust is partly
404 associated with the firework emissions because they cause soil dust resuspension. Factor 4 was
405 coal combustion, characterized by high Zn, As, Se, Hg and Cl^-; it has also a moderate loading of
406 OC and EC. As well known, Hg, As, Se and Zn originate from coal combustion (Feng et al., 2016;
407 Huang et al., 2012; Wang et al., 2010). This factor contributed with 11.5% to the $PM_{2.5}$. Compared
408 to E1, a reduction of approximately 10% was found for coal combustion during E2; this is
409 attributed to the decline in industrial activities during the SF. Factor 5 is termed firework
410 emissions, as it is characterized by high Cl^-, SO_4^{2-}, Mg^{2+}, OC, EC, K and Ba (Huang et al., 2012;
411 Kong et al., 2015; Yang et al., 2014); it contributed with 30% to the $PM_{2..5}$. This factor stood out
412 as the most significant contributor. Factor 6 might be associated with oil combustion for
413 residential heating, as it is characterized by high V and Ni. This factor accounted with 9.3% to the
414 $PM_{2.5}$.

415 The source profiles of the six factors and their contributions for E3 are presented in Fig. 7.
416 Factor 1 could be categorized as vehicle exhaust since it has elevated levels of OC and EC. NO_3^-
417 and NH_4^+ also have some moderate contribution to factor 1. Vehicle exhaust contributed with 32%
418 to the $PM_{2.5}$ during E3. Factor 2 was coal combustion as it is characterized by high loadings of OC,
419 Cl^- and EC (Zhang et al., 2013; Liu et al., 2017b); it accounted for 13.4% of the $PM_{2.5}$. Factor 3
420 was oil combustion characterized by high Ni and V loadings and it accounted for 4.3% of the
421 $PM_{2.5}$. Factor 4 is considered as an industrial source, since it is characterized by high Cr, Mn, Fe,
422 Cu, and Zn. It contributed with 5.2% to the $PM_{2.5}$ whereas no industrial source was present for E2;
423 its presence in E3 is attributed to the re-opening of most industrial factories. Factor 5 was
424 secondary sources, characterized by NO_3^-, SO_4^{2-} and NH_4^+; it accounted for 44% of the $PM_{2.5}$.
425 Factor 6 could be considered as biomass burning and waste incineration, because of the high K

loading. Moderate loadings of As, Se, Hg and Pb are also seen in this factor. This factor contributed with 1.6% to the $PM_{2.5}$.

As shown in Fig. 8, substantial differences in source contributions between the three episodes were found. The vehicle contribution was highest (35%) during E1; firework emissions were most important during E2, when they provided a contribution of 30%, while the secondary source was the largest contributor (44%) during E3. The hourly contribution of the different sources during the episodes is shown in Figs. S6, S7 and S8; the patterns are consistent with the emission sources that were identified above. Finally, an analysis based on chemical mass closure was also used for apportioning the particulate matter to its components; this work is given in the Supplementary material (Figs. S9 and S10).

Conclusions

An intensive observation campaign was organized to study the air quality in urban Beijing during the 2015 SF. $PM_{2.5}$ and its chemical species, including water-soluble inorganic ions, carbonaceous species and trace elements were measured with 1-h time resolution. Based on the chemical characterization and source apportionment analysis, the following conclusions can be drawn:

(1) During the Spring Festival period the changes in anthropogenic activities played an important role in the variation in air pollutants and severe pollution episodes occurred frequently. Before the SF, the higher concentrations of CO, NO_2 and $PM_{2.5}$ were related to a combined effect of unfavorable meteorological conditions, heavy traffic, and residential heating. During the SF the firework emissions gave rise to a steep increase in $PM_{2.5}$ and SO_2 for a short time. After the SF, increased human activities and regional transport contributed a lot to the $PM_{2.5}$ loading.

(2) During the three selected episodes secondary inorganic ions and carbonaceous species accounted for most of the $PM_{2.5}$. Secondary conversion acts a pivotal process in the formation of air pollution. The firework emissions released lots of gaseous pollutants and particles containing harmful chemicals like heavy metals in a short time, posing health risks to tourists and local residents. Thus, more attention should be paid to limit fireworks during the SF.

(3) The results of the source apportionment indicated that vehicle exhaust, fireworks and secondary sources, respectively, were important contributors during the three selected episodes,

which is consistent with the change in emission sources.

This study enhances our understanding of the impact of the change in anthropogenic activities on the characteristics, formation mechanisms, and sources of the air pollution. Based on near real-time data of the chemical composition of the $PM_{2.5}$, the evolution of the air pollution episodes, their dynamical characteristics and the sources could be precisely identified. Future work will focus on developing methods for monitoring more tracers of the different emission sources with high time resolution to improve the accuracy of the source apportionment.

Acknowledgements

This study was supported by the Ministry of Science and Technology of China (2016YFC0202701), the Beijing Municipal Science and Technology Project (D17110900150000) and the Strategic Priority Research Program (B) of the Chinese Academy of Sciences (Grant XDB05020500). The authors thank all staff members of the IAP, CAS for operating and maintaining the analyzers used. In addition, the authors acknowledge helpful discussions with Dr. John Cooper (Cooper Environmental Services, USA).

References

Beijing environmental statement 2015, http://www.bjepb.gov.cn/2015zt_jsxl/index.html

Betha, R., Behera, S. N., Balasubramanian, R., 2014. 2013 Southeast Asian smoke haze: fractionation of particulate-bound elements and associated health risk. Environ. Sci. Technol. 48, 4327-4335.

Cao, J., Wu, F., Chow, J., Lee, S., Li, Y., Chen, S., et al., 2005. Characterization and source apportionment of atmospheric organic and elemental carbon during fall and winter of 2003 in Xi'an, China. Atmos. Chem. Phys. 5, 3127-3137.

Chan, Y. C., Simpson, R. W., Mctainsh, G. H., Vowles, P. D., Cohen, D. D., Bailey, G. M., 1997.Characterisation of chemical species in $PM_{2.5}$ and PM_{10} aerosols in Brisbane, Australia. Atmos. Environ. 31, 3773-3785.

Chang, Y., Zou, Z., Deng, C., Huang, K., Collett, J. L., Lin, J., et al., 2015. The importance of vehicle emissions as a source of atmospheric ammonia in the megacity of Shanghai. Atmos. Chem. Phys. 16, 3577-3594.

Chen, R., Yin, P., Meng, X., Liu, C., Wang, L., Xu, X., et al., 2017. Fine particulate air pollution and daily mortality: a nationwide analysis in 272 Chinese cities. Am. J. Respir. Crit. Care Med. 196, 73-81.

Cheng, N. L., Li, Y. T., Qiu, Q. H., Dong, X., Sun, R. W., 2015. Analysis on spatial and temporal distribution of $PM_{2.5}$ during heavy pollution days in Beijing in 2013. Environ. Monit. China 31, 38-42.

Cohen, A. J., Brauer, M., Burnett, R., Anderson, H. R., Frostad, J., Estep, K., et al., 2017. Estimates and 25-year trends of the global burden of disease attributable to ambient air pollution: an analysis of data from the Global Burden of Diseases Study 2015. The Lancet 389, 1907-1918.

Dall'Osto, M., Querol, X., Amato, F., Karanasiou, A., Lucarelli, F., Nava, S., et al., 2013. Hourly elemental concentrations in $PM_{2.5}$ aerosols sampled simultaneously at urban background and road site during SAPUSS–diurnal variations and PMF receptor modelling. Atmos. Chem. Phys. 13, 4375-4392.

Dong, D. B., Zhu, S., Rui, B., 2014. Evolution Characteristics of $PM_{2.5}$ Mass Concentration During 2013 Spring Festival in Hefei. J Atmos. Environ. Optics 9, 268-274.

Elser, M., Huang, R. J., Wolf, R., Slowik, J. G., Wang, Q. Y., Canonaco, F., et al., 2016. New insights into $PM_{2.5}$ chemical composition and sources in two major cities in China during extreme haze events using aerosol mass spectrometry. Atmos. Chem. Phys. 16, 3207-3225.

Feng, J., Yu, H., Su, X., Liu, S., Li, Y., Pan, Y., et al., 2016. Chemical composition and source apportionment of $PM_{2.5}$ during Chinese Spring Festival at Xinxiang, a heavily polluted city in North China: Fireworks and health risks. Atmos. Res. 182, 176-188.

Gao, J., Peng, X., Chen, G., Xu, J., Shi, G.-L., Zhang, Y.-C., et al., 2016. Insights into the chemical characterization and sources of PM2.5 in Beijing at a 1-h time resolution. Sci. Total Environ. 542, 162-171.

Guo, H., Wang, Y., Zhang, H., 2017. Characterization of criteria air pollutants in Beijing during 2014–2015. Environ. Res. 154, 334-344.

Hamad, S., Green, D., Heo, J., 2016. Evaluation of health risk associated with fireworks activity at Central London. Air Qual. Atmos. Health 9, 735-741.

Han, F., Kota, S. H., Wang, Y., Zhang, H., 2017. Source apportionment of PM2.5 in Baton Rouge, Louisiana during 2009–2014. Sci. Total Environ. 586, 115-126.

Han, S., Bian, H., Feng, Y., Liu, A., Li, X., Zeng, F., et al., 2011. Analysis of the Relationship between O_3, NO and NO_2 in Tianjin, China. Aerosol Air Qual. Res. 11, 128-139.

Hu, J., Ying, Q., Wang, Y., Zhang, H., 2015a.Characterizing multi-pollutant air pollution in China: Comparison of three air quality indices. Environ. Int. 84, 17-25.

Hu, J., Wu, L., Zheng, B., Zhang, Q., He, K., Chang, Q., et al., 2015b. Source contributions and regional transport of primary particulate matter in China. Environ. Pollut. 207, 31-42.

Huang, K., Zhuang, G., Lin, Y., Wang, Q., Fu, J. S., Zhang, R., et al., 2012. Impact of anthropogenic emission on air quality over a megacity–revealed from an intensive atmospheric campaign during the Chinese Spring Festival. Atmos. Chem. Phys. 12, 11631-11645.

Jeong, C.-H., Wang, J. M., Evans, G. J., 2016. Source apportionment of urban particulate matter using hourly resolved trace metals, organics, and inorganic aerosol components. Atmos. Chem. Phys. Discuss., doi:10.5194/acp-2016-189.

Ji, D., Wang, Y., Wang, L., Chen, L., Hu, B., Tang, G., et al., 2012. Analysis of heavy pollution episodes in selected cities of northern China. Atmos. Environ. 50, 338-348.

Ji, D., Zhang, J., He, J., Wang, X., Pang, B., Liu, Z., et al., 2016. Characteristics of atmospheric organic and elemental carbon aerosols in urban Beijing, China. Atmos. Environ. 125, 293-306.

Ji, D., Li, L., Pang, B., Xue, P., Wang, L., Wu, Y., et al., 2017. Characterization of black carbon in an urban-rural fringe area of Beijing. Environ. Pollut. 223, 524-534.

Jia, Y., Stone, D., Wang, W., Schrlau, J., Tao, S., Simonich, S. L., 2011. Estimated reduction in cancer risk due to PAH exposures if source control measures during the 2008 Beijing Olympics were sustained. Environ. Health Perspect. 119, 815.

Jin, J., Wang, Y., Li, L., Li, J., Wei, Q., 2007. Particles pollution and impact caused by fireworks in Beijing during Spring Festival. Environ. Pollut. Cont. 29, 229-232.

Kong, S., Li, L., Li, X., Yin, Y., Chen, K., Liu, D., et al., 2015. The impacts of firework burning at the Chinese Spring Festival on air quality: insights of tracers, source evolution and aging processes. Atmos. Chem. Phys. 15, 2167-2184.

Lin, H., Liu, T., Xiao, J., Zeng, W., Li, X., Guo, L., et al., 2016. Mortality burden of ambient fine particulate air pollution in six Chinese cities: results from the Pearl River Delta study. Environ. Int. 96, 91-97.

Liu, B., Wu, J., Zhang, J., Wang, L., Yang, J., Liang, D., et al., 2017a. Characterization and source

apportionment of PM2.5 based on error estimation from EPA PMF 5.0 model at a medium city in China. Environ. Pollut. 222, 10-22.

Liu, B., Yang, J., Yuan, J., Wang, J., Dai, Q., Li, T., et al., 2017b. Source apportionment of atmospheric pollutants based on the online data by using PMF and ME2 models at a megacity, China. Atmos. Res. 185, 22-31.

Liu, J., Man, Y., Liu, Y., 2014a. Temporal variability of PM_{10} and $PM_{2.5}$ inside and outside a residential home during 2014 Chinese Spring Festival in Zhengzhou, China. Nat Hazards 73, 2149-2154.

Liu, T., Zhang, Y. H., Xu, Y. J., Lin, H. L., Xu, X. J., Luo, Y., et al., 2014. The effects of dust–haze on mortality are modified by seasons and individual characteristics in Guangzhou, China. Environ. Pollut. 187, 116-123.

Norris, G. A., Duvall, R., Brown, S. G., Bai, S., 2014. EPA Positive Matrix Factorization (PMF) 5.0 fundamentals and User Guide Prepared for the US Environmental Protection Agency Office of Research and Development, Washington, DC. DC EPA/600/R-14/108.

Pathak, R. K., Wu, W. S., Wang, T., 2009. Summertime $PM_{2.5}$ ionic species in four major cities of China: nitrate formation in an ammonia-deficient atmosphere. Atmos. Chem. Phys. 9, 1711-1722.

Perry, K. D., 1999.Effects of outdoor pyrotechnic displays on the regional air quality of Western Washington State. J. Air Waste Manage. Assoc. 49, 146-155.

Pokorná, P., Hovorka, J., Hopke, P. K., 2016. Elemental composition and source identification of very fine aerosol particles in a European air pollution hot-spot. Atmos. Pollut. Res. 7, 671-679.

Shen, Z., Sun, J., Cao, J., Zhang, L., Zhang, Q., Lei, Y., et al., 2016. Chemical profiles of urban fugitive dust $PM_{2.5}$ samples in Northern Chinese cities. Sci. Total Environ. 569, 619-626.

Singh, A., Rastogi, N., Patel, A., Singh, D., 2016. Seasonality in size-segregated ionic composition of ambient particulate pollutants over the Indo-Gangetic Plain: Source apportionment using PMF. Environ. Pollut. 219, 906-915.

Tao, J., Ho, K.-F., Chen, L., Zhu, L., Han, J., Xu, Z., 2009. Effect of chemical composition of PM 2.5 on visibility in Guangzhou, China, 2007 spring. Particuology 7, 68-75.

Tian, Y., Wang, J., Peng, X., Shi, G., Feng, Y., 2014. Estimation of the direct and indirect impacts of fireworks on the physicochemical characteristics of atmospheric PM_{10} and $PM_{2.5}$. Atmos. Chem. Phys. 14, 9469-9479.

573 Wang, G., Cheng, S., Wei, W., Yang, X., Wang, X., Jia, J., et al., 2017. Characteristics and
574 emission-reduction measures evaluation of $PM_{2.5}$ during the two major events: APEC and Parade.
575 Sci. Total Environ. 595, 81-92.
576 Wang, S., Zhang, L., Li, G., Wu, Y., Hao, J., Pirrone, N., et al., 2010. Mercury emission and
577 speciation of coal-fired power plants in China. Atmos. Chem. Phys. 10, 1183-1192.
578 Wang, Y., Zhang, Y., Schauer, J. J., de Foy, B., Guo, B., Zhang, Y., 2016. Relative impact of
579 emissions controls and meteorology on air pollution mitigation associated with the Asia-Pacific
580 Economic Cooperation (APEC) conference in Beijing, China. Sci. Total Environ. 571, 1467-1476.
581 Wang, Z., Zhang, D., Li, Y., Feng, P., Dong, X., Sun, R., et al., 2015. Analysis of air quality in
582 Beijing City during Spring Festival period of 2014. Acta Scientiae Circumstantiae 35, 371-378.
583 Wei, F., Yang, Z., Jiang, D., Liu, Z., Sun, B., 1991. Basic statistics and features for background
584 values of soil elements in China. Environ. Monit. China 7, 1-6.
585 Wen, T., Wang, Y., Chang, S.-Y., Liu, G., 2006. On-line measurement of water-soluble ions in
586 ambient particles. Adv. Atmos. Sci. 23, 586-592.
587 Xie, Y., Zhao, B., Zhao, Y., Luo, Q., Wang, S., Zhao, B., et al., 2017. Reduction in population
588 exposure to $PM_{2.5}$ and cancer risk due to $PM_{2.5}$-bound PAHs exposure in Beijing, China during the
589 APEC meeting. Environ. Pollut. 225, 338-345.
590 Xu, L., Yu, Y., Yu, J., Chen, J., Niu, Z., Yin, L., et al., 2013. Spatial distribution and sources
591 identification of elements in $PM_{2.5}$ among the coastal city group in the Western Taiwan Strait
592 region, China. Sci. Total Environ. 442, 77-85.
593 Yang, L., Gao, X., Wang, X., Nie, W., Wang, J., Gao, R., et al., 2014. Impacts of firecracker burning
594 on aerosol chemical characteristics and human health risk levels during the Chinese New Year
595 Celebration in Jinan, China. Sci. Total Environ. 476, 57-64.
596 Yao, L., Yang, L., Yuan, Q., Yan, C., Dong, C., Meng, C., et al., 2016. Sources apportionment of
597 PM 2.5 in a background site in the North China Plain. Sci. Total Environ. 541, 590-598.
598 Yu, L., Wang, G., Zhang, R., Zhang, L., Song, Y., Wu, B., et al., 2013. Characterization and source
599 apportionment of $PM_{2.5}$ in an urban environment in Beijing. Aerosol Air Qual. Res. 13, 574-583.
600 Zíková, N., Wang, Y., Yang, F., Li, X., Tian, M., Hopke, P. K., 2016. On the source contribution to
601 Beijing $PM_{2.5}$ concentrations. Atmos. Environ. 134, 84-95.
602 Zhang, R., Jing, J., Tao, J., Hsu, S. C., 2013. Chemical characterization and source apportionment of

$PM_{2.5}$ in Beijing: seasonal perspective. Atmos. Chem. Phys. 13, 7053-7074.

Zhang, Y., Huang, W., Cai, T., Fang, D., Wang, Y., Song, J., et al., 2016. Concentrations and chemical compositions of fine particles ($PM_{2.5}$) during haze and non-haze days in Beijing. Atmos. Res. 174, 62-69.

Zong, Z., Wang, X., Tian, C., Chen, Y., Qu, L., Ji, L., et al., 2016. Source apportionment of PM2.5 at a regional background site in North China using PMF linked with radiocarbon analysis: insight into the contribution of biomass burning. Atmos. Chem. Phys. 16, 11249-11265.

Zou, Q., Yao, Y. G., 2014. The analysis of characteristics of $PM_{2.5}$ components during set-off fireworks period of spring festival in Suzhou city. Environ. Monit. China 30, 100-106.

Table 1 Average concentrations and associated standard deviations of $PM_{2.5}$ (μg/m^3) as well as of water-soluble inorganic ions, carbonaceous species (μg/m^3) and trace elements (ng/m^3) in $PM_{2.5}$ during the three selected episodes of the study period.

Species	E1	E2	E3
$PM_{2.5}$	107±70	102±99	72±76
Water-soluble inorganic ions			
Cl^-	5.2±3.2	11.5±15.2	2.6±2.2
NO_3^-	18±12	9.9±9.0	12±13
SO_4^{2-}	11±6.1	23±25	15±16
Na^+	1.8±0.3	1.4±0.4	1.6±0.3
K^+	1.0±0.6	18±25	1.2±1.2
NH_4^+	11±6.7	7.3±8.1	12±14
Mg^{2+}	0.1±0.0	1.1±1.7	0.1±0.0
Carbonaceous species			
OC	26±16	14±12	13±9.7
EC	3.8±2.4	1.9±1.7	1.6±1.4
Trace elements			
K	1350±370	1350±1100	410±172
Ca	158±49	156±119	34±18
V	5.7±10	16±7.7	7.1±7.0
Cr	3.0±2.1	0.5±0.8	0.4±0.6
Mn	29±12	10±4.7	4.1±2.6
Fe	360±110	250±130	87±40
Ni	3.0±2.6	5.8±2.1	3.2±2.7
Cu	44±23	11±6.2	5.1±2.0
Zn	240±100	45±18	36±19
As	29±10	8.1±2.6	2.3±3.3
Se	5.3±1.4	2.0±0.8	0.6±0.4
Ag	6.8±3.7	7.8±3.0	6.7±2.5
Cd	11±3.1	11±3.2	9.9±2.5
Ba	32±11	59±65	9.6±5.6
Hg	3.6±0.7	2.7±1.0	1.5±0.3
Pb	98±26	39±15	18±14

Figure
Click here to download Figure: Figs_20171115.docx

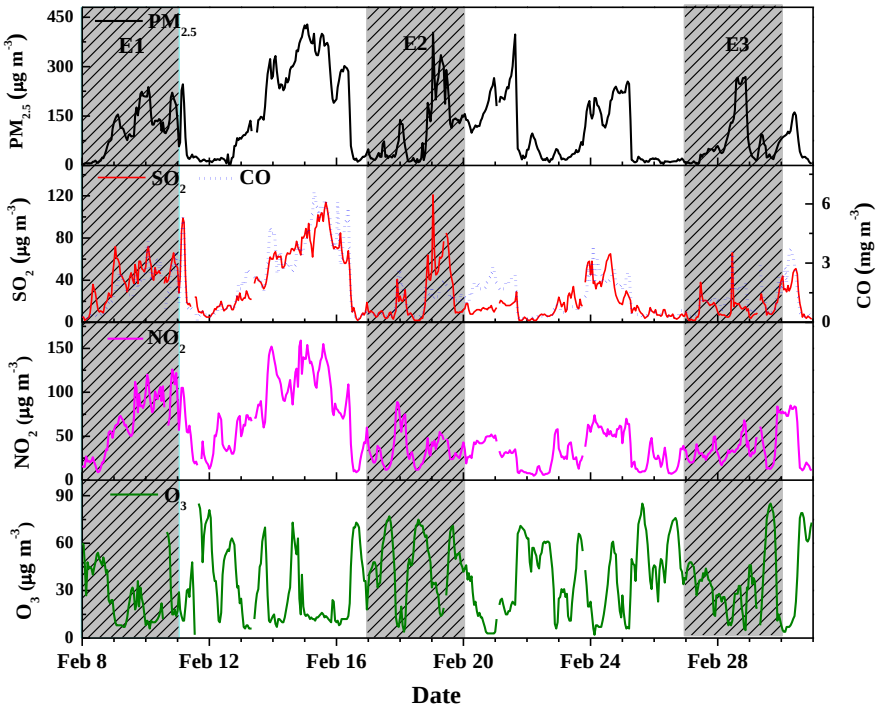

(a)

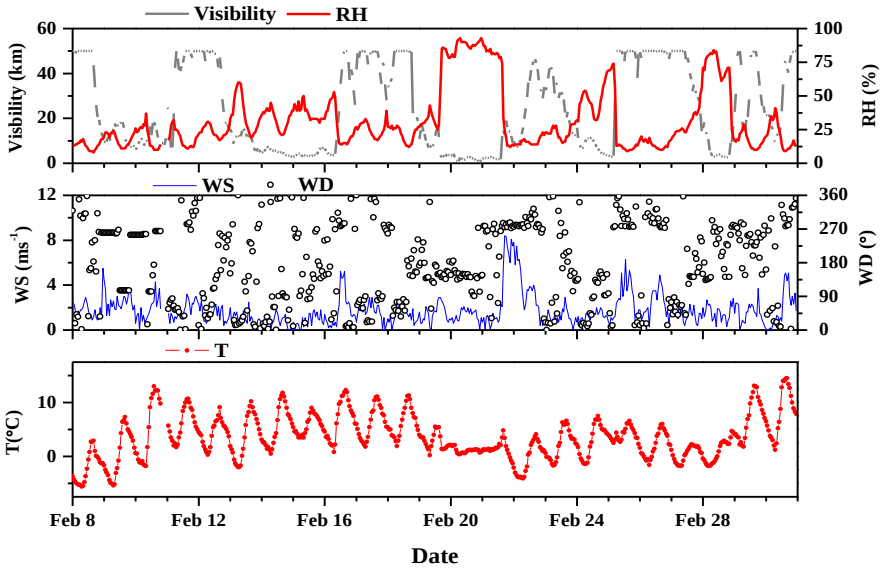

(b)

Fig. 1 Hourly $PM_{2.5}$ and SO_2, CO, NO_2 and O_3 (a) and time series of visibility, relative humidity, wind speed, wind direction and temperature (b) from February 8 to March 2, 2015 at the observation site.

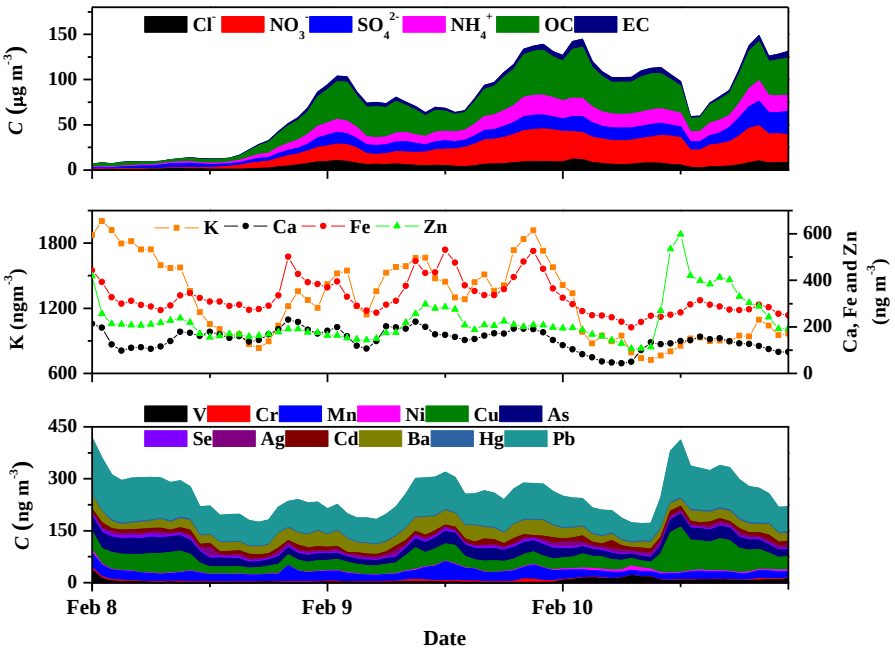

Fig. 2 Hourly concentrations of chemical species in $PM_{2.5}$ during E1.

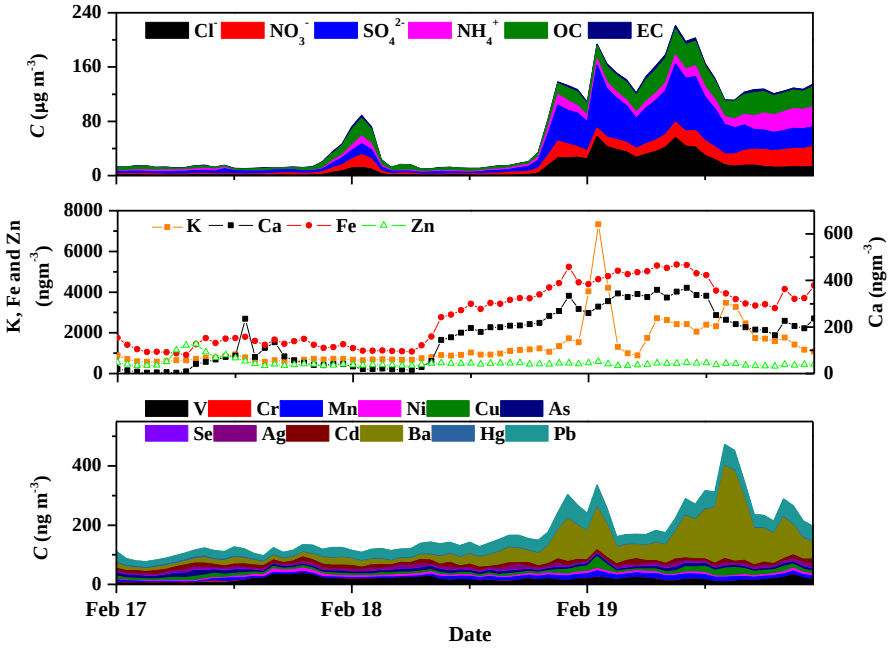

Fig. 3 Hourly concentrations of chemical species in $PM_{2.5}$ during E2.

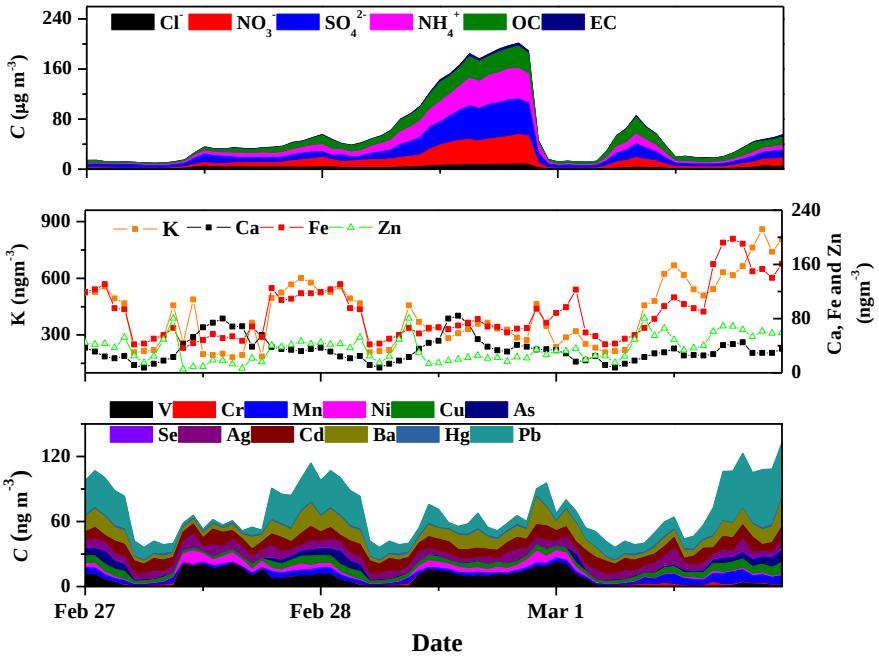

Fig. 4 Hourly concentrations of chemical species in $PM_{2.5}$ during E3.

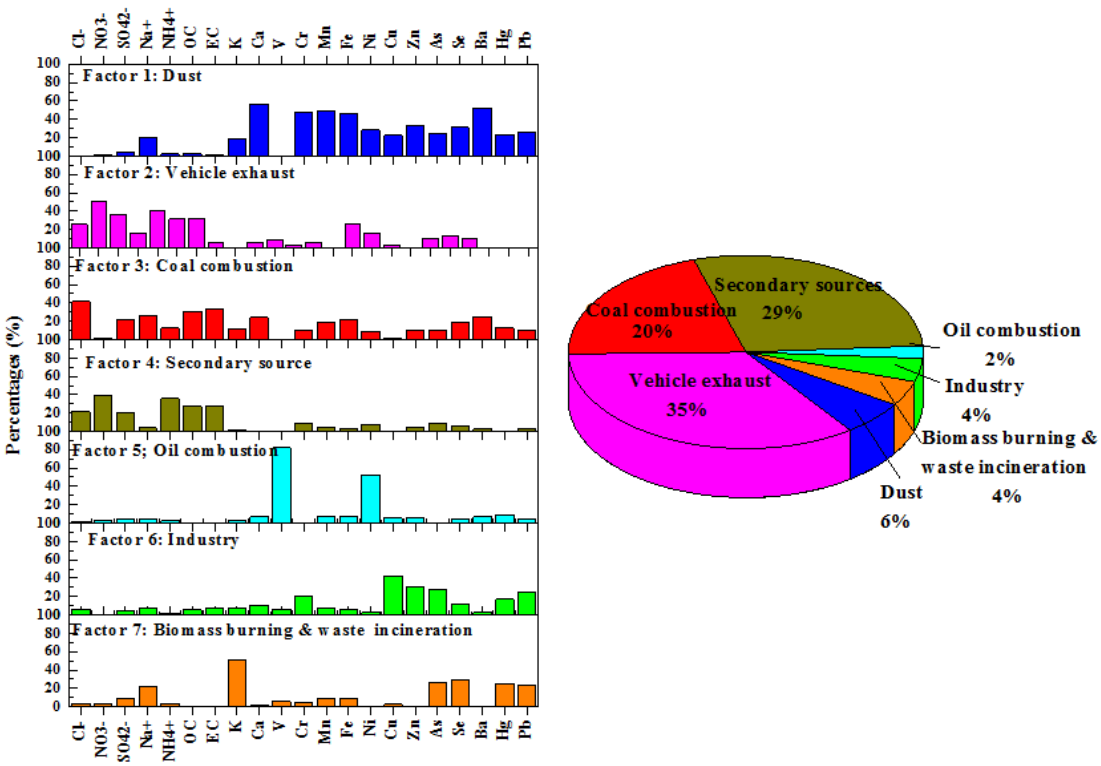

Fig. 5 Profile and contribution of each source during E1.

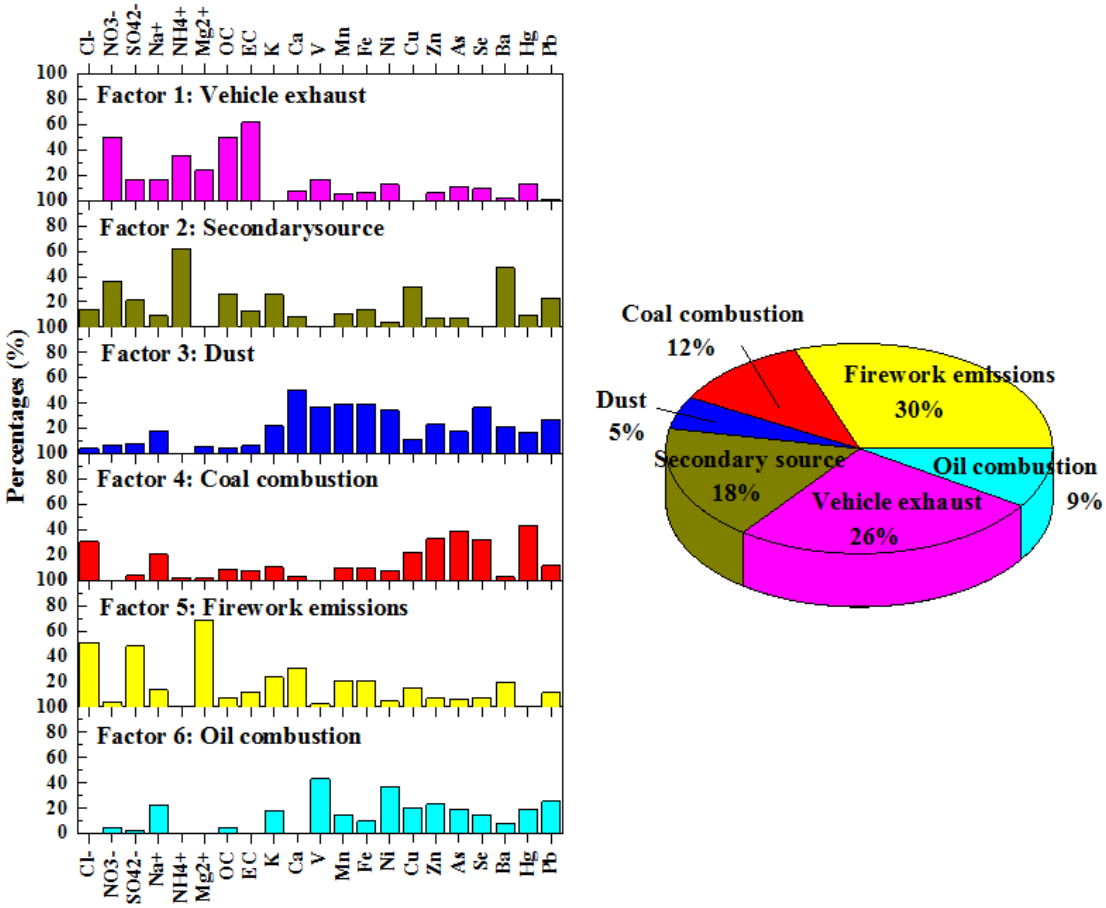

Fig. 6 Profiles and contribution of each source during E2.

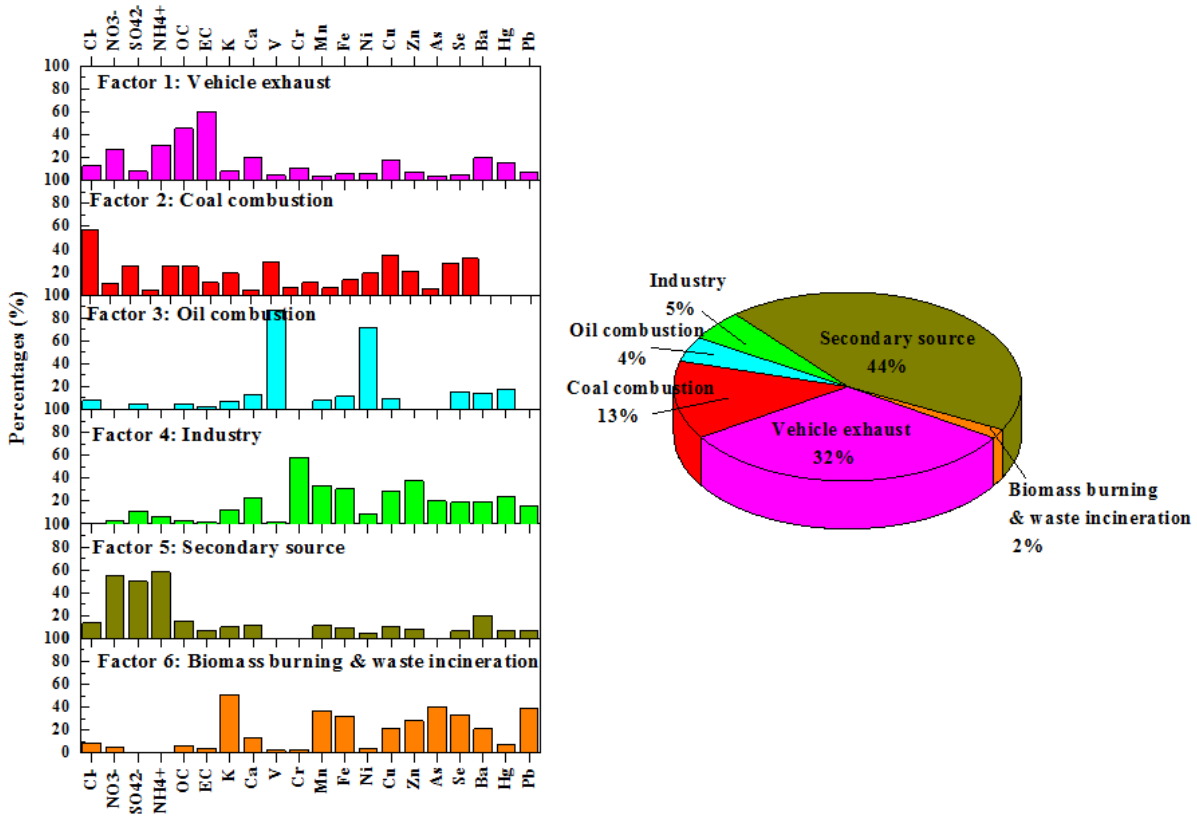

Fig. 7 Profile and contribution of each source during E3.

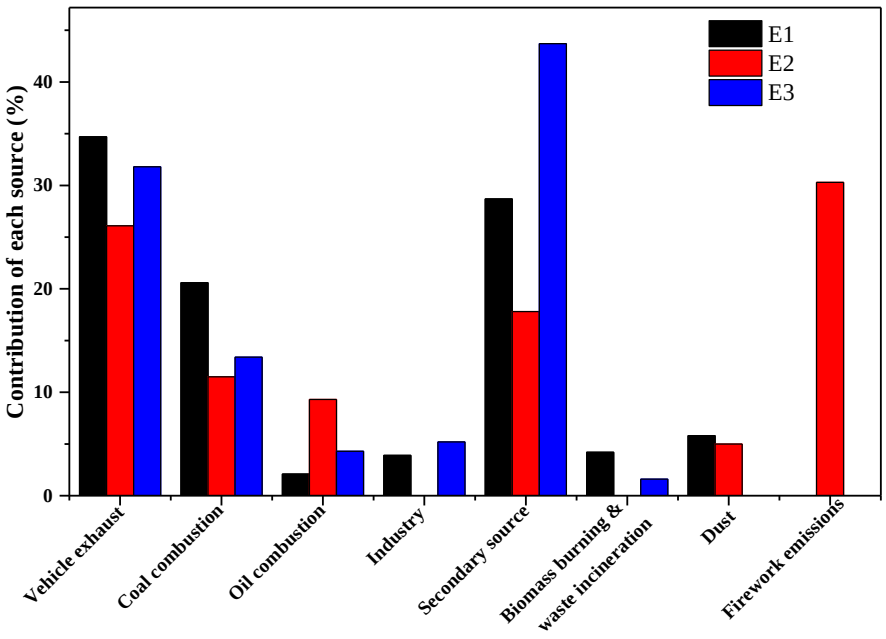

Fig. 8 Comparison of source contributions during the three selected pollution episodes.

Supplementary material for on-line publication only

Click here to download Supplementary material for on-line publication only: Supplementary materials_20171115.docx